Eur. Phys. J. Plus (2022) 137:1371
https://doi.org/10.1140/epjp/s13360-022-03599-2

THE EUROPEAN PHYSICAL JOURNAL PLUS

Regular Article

Growth of zinc oxide thin films using different precursor solutions by spray pyrolysis technique

Asmaa Al-Rasheedi[1], Akhalakur Rahman Ansari[2], A. M. Abdeldaim[1,3], M. S. Aida[1,a]

[1] Physics department Faculty of Science, King Abdulaziz University, Jeddah, Saudi Arabia
[2] Center on Nanotechnology, King Abdulaziz University, Jeddah, Saudi Arabia
[3] Physics Department, Faculty of Science, Zagazig University, Zagazig, Egypt

Received: 24 July 2022 / Accepted: 14 December 2022

Abstract The present paper deals with the influence of precursor salt source on the properties of zinc oxide (ZnO) thin films prepared by spray pyrolysis. For this purpose, three zinc salt sources were studied including zinc acetate, zinc chloride, and zinc nitrate. X-ray diffraction (XRD), scanning electron microscopy (SEM), and optical transmittance spectra were used to investigate the structural and optical properties of ZnO thin films. Regardless the used precursor, ZnO thin films have the Wurtzite hexagonal crystallographic phase. SEM images reveal that the ZnO thin films surface morphology strongly governed by the precursor source nature. ZnO thin films prepared with zinc acetate salt are smooth, highly transparent and composed of small particle size. While, films prepared with zinc chloride are dense, owing a good crystallinity with a high texturation along (002) and rough surface film with larger particle size. The effect of solution salt is explained in term of the difference in the viscosity and the surface tension of the used solution. We inferred that high viscosity and surface tension solution such as the prepared one with zinc chloride, hinder the droplet motion on substrate surface in contrary to the solution prepared with zinc acetate. The PL emission spectra of films recorded at room temperature in the wavelength range 340–800 nm indicated that the salt solution has less effect on the electronic defects in the synthetized ZnO thin films.

1 Introduction

Nowadays ZnO thin films have emerged as one of promising metallic oxide semiconductor. Due to their unique and interesting semiconducting properties such as: nontoxicity, abundance, chemical stability, wide direct band gap (3.27 eV), large excitonic bonding (60 meV, n-type conductivity, good piezoelectricity and transparency, ZnO is suitable for use in optoelectronic devices [1]. Therefore, ZnO is recommended for several applications including sensors [1], surface acoustic devices [2], transparent electrodes [3], and solar cells [4],

ZnO thin films were prepared by several techniques such as sputtering [5], thermal evaporation [6], electrodeposition [7], sol gel [8], pulsed laser deposition [9], metal–organic chemical vapor deposition and spray pyrolysis [10]. Among these, spray pyrolysis has been extensively studied, due to the fact that it is a simple, inexpensive and environmental friendly technique. Spray pyrolysis is the most economic and versatile technique for deposition of metal oxides, it has numerous advantage [11].

It is well-known that the film properties are close related to the used deposition technique on one hand and to the specific deposition parameters of the adopted technique on the other hand. Spray pyrolysis method has been used for large number of metallic oxide thin films namely ZnO, SnO_2, MgO, In_2O_3, TiO_2, CuO …etc. deposition. The influence of the deposition parameters influence on sprayed ZnO thin films properties has been investigated in the literature. Substrate temperature [12], solution molarity [13], flow rate [14], annealing [15] and doping [16] were intensively studied. However, very few reports were devoted to the study of the zinc salt nature. Bacaksiz et al. [17] have deposited ZnO thin film with different solution precursors, they concluded that the nature of salt source controls the structural and optical proprieties of ZnO thin films. Khammar et al. [18] studied the effect of the properties of starting solution on ZnO thin films prepared by ultrasonic spray. Recently, Baig et al. [19] investigated the influence of solvents on doped ZnO thin films properties, they concluded that the solution properties alter the spin coated thin film properties as well. The spray deposition technique is solution based. The generated droplets, by air pressure (pneumatic spray) or by ultrasound vibration (ultrasonic spray), are sprayed onto a heated surface where they react to form a solid film. During their landing on substrate, the droplets motion on the heated substrate is governed by the fluid mechanics laws. Lower surface tension and viscosity of the solution favors the easy the droplet spreading. Whilst, solution owing large surface tension and viscosity hinder

[a] e-mail: aida_salah2@yahoo.fr (corresponding author)

Published online: 25 December 2022

the droplet spreading. Thereafter, the properties of the used solution including the solution viscosity and surface tension play a key role on the droplet dynamic and consequently on the resulting film morphology [18].

To the best to our knowledge, there is no investigations dealing with the effect of starting solution properties on ZnO thin films prepared by pneumatic spray pyrolysis.

In this study, we report the effects of different precursor's source such as zinc acetate, zinc chloride, and zinc nitrate on the properties of ZnO thin films prepared by pneumatic spray pyrolysis.

2 Experimental details

ZnO thin films preparation by spray pyrolysis, three zinc salts namely zinc acetate, zinc nitrate, and zinc chloride are used in the present study (purchased from Sigma-Aldrich with a purity of 99.9995%). The starting solutions were prepared by dissolving the salt source in distilled water to obtain a solution of 0.1 molarity. The films were deposited on well cleaned glass substrate at a substrate temperature of 400 °C with a flow rate of 0.014 ml/s during 1 min of deposition time.

In order to correlate the ZnO thin films structure to the solution physical parameters, both the surface tension and the viscosity of the utilized solutions are measured.

A Ubbelohde type viscometer was used to measure the viscosity of the aqueous solutions. Before measuring, the used vessel was cleaned and rinsed with methanol rinse to eliminate any contaminants that may obstruct the liquid dynamic during the measurement. The surface tension of the used three solution was measured by means Dunouy tensiometer. The force required to remove a platinum ring immersed in the solution is used to calculate surface tension. Before each measurement, the ring was carefully cleaned and dried.

The structural properties of the films were analyzed by XRD diffractometer Ultima-IV Rigaku system with Cu K_α radiation (λ_{Cu} = 0.154056 nm) working at 40 kV of accelerating voltage and 40 mA of current. The 2θ value was varied in the range from 20º to 80º. The film's morphology was investigated by means of field emission SEM (JSM–7600F JEOL). The optical properties of the synthetized films were studied using transmission measurements performed using Perkin Elmer Lambda750 spectrophotometer in the UV–visible range (200–2000 nm).

The thickness and refractive index of films were evaluated by fitting the transmission data. In this procedure, the experimental transmittance data are fitted with the theoretical one deduced form Swanepoel theory [20]. In this approach, the film thickness and refractive index are varied till convergence.

The photoluminescence (PL) measurements, recorded in the range 350 and 850 nm, were carried out using spectrofluorometer Horiba with a Xe lamp with 325 nm excitation wavelength as the excitation light source at room temperature.

3 Results and discussion

3.1 Structural properties

The XRD spectra of ZnO thin films synthesized on glass substrate at 400 °C using zinc chloride (Fig. 1a), zinc nitrate (Fig. 1b), and zinc acetate (Fig. 1c) as ZnO precursors are shown in Fig. 1. As can be seen, the film's microstructure is highly influenced by the type of precursor utilized. The diffraction pattern of different films is composed of several peaks indicating their polycrystalline nature. Peaks are respectively assigned to the diffraction plane (100), (002), (101), (120), (102), (110), (103) and (112) of the ZnO Wurtzite phase ((JCPDS card 6-0416). There are no diffraction peaks of any other impurity phases in all samples. The film prepared with chloride zinc salt exhibits a preferential orientation along (002) suggesting its growth along the c axis normal to the surface substrate. However, films prepared with acetate and nitrate salt have a lesser preferential growth along the (002) plane. The same conclusion has been outlined by Lehraki et al. [13] in ZnO thin films prepared by ultrasonic spray pyrolysis with different zinc salt source.

The texturation coefficient of (*hkl*) peak noticed TC (*hkl*), informing about its preferential orientation degree, can be evaluated from the peak intensities using Harris method [21] in polycrystalline material expressed by following equation:

$$\mathrm{TC}(hkl) = \frac{I(hkl)/I_0(hkl)}{N_r^{-1}\sum_{N_r}\frac{I(hkl)}{I_0}(hkl)}$$

where *I(hkl)* and $I_0(hkl)$ are relative intensities of the measured and the corresponding peak from the powder reference of the peak *(hkl)* respectively and *Nr* is the number of peaks.

The calculated texturation coefficient of the most encountered peaks in ZnO thin film i.e. (100), (002) and (101) are plotted in Fig. 2. As shown the film prepared with zinc chloride salt has a highly preferential orientation along the direction (002). While films prepared with acetate and nitride do not exhibit a clear preferential orientation.

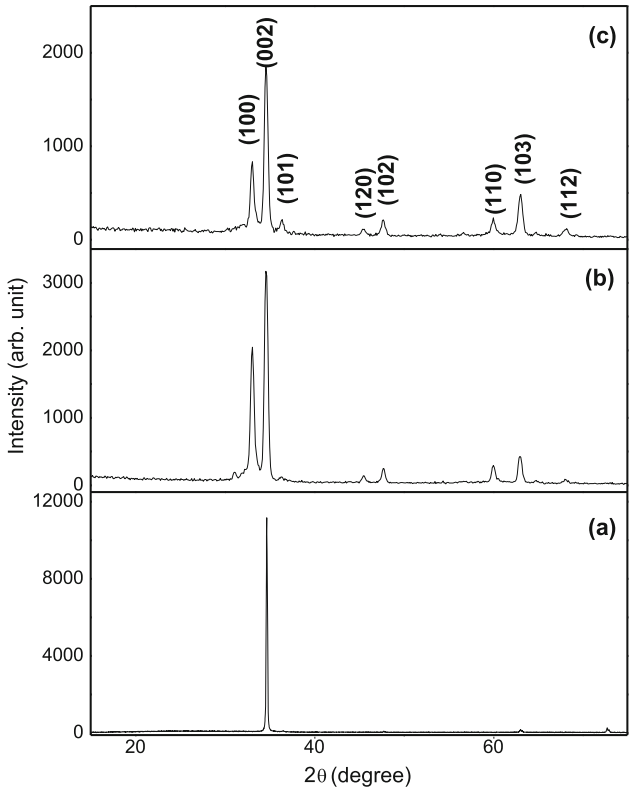

Fig. 1 XRD pattern of ZnO films deposited with different solutions. **a** Zinc chloride, **b** Zinc nitride and **c** Zinc acetate

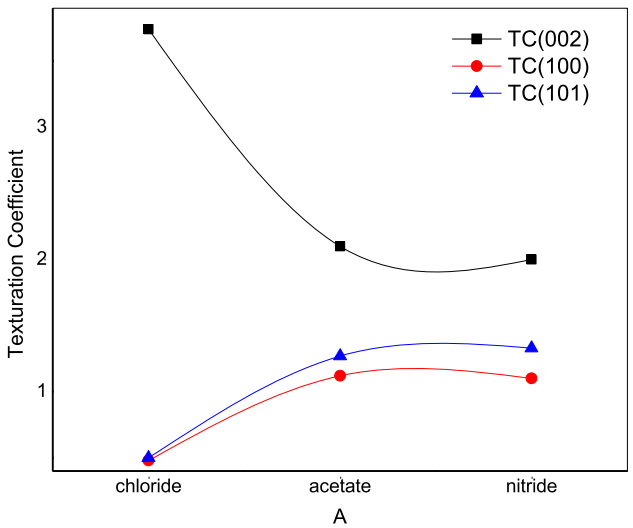

Fig. 2 Texturation coefficient of the three peaks (002), (100) and (101) in films prepared with the three studied salts

The lattice parameter of different films is calculated using the the expression given by Eq. (1) [22]:

$$\frac{1}{d^2} = \frac{4}{3}\left(\frac{h^2 + hk + k^2}{a^2}\right) + \frac{l^2}{c^2} \tag{1}$$

where a and c are the lattice parameters, d is the inter-plane spacing and the Miller indices are denoted by h, k, and l.

The standard Bragg relation (Eq. (2)) is used to calculate the inter-planar spacing (d) [23]:

$$d = \frac{n\lambda}{2\sin\theta} \tag{2}$$

where λ is the X-ray wavelength (1.5418 Å) and θ is the diffraction angle.

The calculated parameters of different films are regrouped in Table 1. The obtained values are in good agreement with ASTM data. The c parameter values of all ZnO films are less than the value of bulk ZnO [24], which is 0.5206 nm, indicating that our films

Table 1 Calculated parameters of ZnO thin films prepared at different salts

Solution	2θ (°)	*hkl* planes	d (Å)	a (Å)	c (Å)	$v_{\text{unit cell}}$ (Å)^3	D (nm)	cosθ	β	δ (10^{15}lines/m^2)	ε (10^{-3})
Chloride	34.62	(002)	2.590	3.18	5.18	45.36	17.2	0.9547	0.484	3.38	2.000
Nitrate	34.49	(002)	2.600	3.19	5.20	45.83	14.7	0.9550	0.564	4.63	2.360
Acetate	34.66	(002)	2.585	3.17	5.17	45.04	14.8	0.9546	0.562	4.57	2.347

are subjected to compressive stress along the c axis. The changes in lattice parameter values that result is related to the intrinsic stress that develops in the ZnO crystal lattice.

The Debye-Scherer equation [25] was used to calculate the crystallite size D of the film:

$$D = \frac{0.9\lambda}{\beta \cos\theta} \tag{3}$$

where λ is the used X rays radiation wavelength (0.15418 nm), θ and β are respectively the diffraction angle and the full width at half maximum (FWHM) of the selected diffraction peak.

Knowing the crystallite size D, the dislocation density (δ) was calculate using the Williamson and Smallman [25] formula (Eq. (4)):

$$\delta = \frac{1}{D^2} \tag{4}$$

the micro strains (ε) in the films was evaluated by using the following equations [26]

$$\varepsilon = \frac{\beta \cos\theta}{4} \tag{5}$$

In Table 1, we have regrouped the calculated values of lattice constant (a), inter-planar spacing (d) crystallite size, dislocation and strain in ZnO thin films prepared with the three used salts source precursors. As can be deduced from Table 1, the film synthetized with zinc chloride exhibits low micros strain and less dislocation density by comparison to their values in the films obtained by the two other salt sources. The reduction in the strain is consistent with the observed preferential orientation in the film prepared with chloride salt. The preferred orientation is known to be due to the internal stress and surface energy reduction [27].

3.2 Surface morphology

SEM images of ZnO thin films prepared with zinc chloride, zinc nitrate and zinc acetate as precursors are shown in Fig. 3a–c. As can be seen, the films have different surface morphologies indicating that the slat source plays a crucial role on the film morphology. The zinc chloride film (Fig. 3a) has rough surface morphologies, whereas the zinc nitrate (Fig. 3b) and zinc acetate (Fig. 3c) film have a continuous and smooth appearance. The grain size, deduced from SEM images, depends on the used salt source, in Table 2 is regrouped the grain size values in different films.

As mentioned above, spray pyrolysis films formation is aqueous solution based. The film formation passes through three steps: (i) solution atomization to generate fine droplets (ii) droplets spraying on heated surface (iii) surface reactions. Each step may have an impact on the properties of the future formed film. During their arrival on the substrate, the droplets dynamic is governed by the solution properties namely the viscosity and surface tension. These two quantities are at the origin of the resistance hindering the droplet motion and spreading onto substrate surface. They control, thereafter, the droplet spreading and flattening on the substrate surface and consequently the nucleation step during the film formation.

In order to explain, the influence of the salt source on the films structural and morphological properties of the synthetized ZnO films, we have measured the salt solution properties and correlate them with the film's properties. In Table 2 is reported the surface tension and viscosity of the various studied salts solution. Chloride zinc salt has a higher surface tension and viscosity regarding the two other salt sources.

Since, chloride zinc salt has the largest surface tension and viscosity (Table 2), the incoming droplets cannot easily spread on the substrate surface. Consequently, these favors, the film vertical growth (along the c axis) and leads to rough film with larger grain size as deduced from XRD analysis and SEM observation. However, when using zinc acetate or nitride precursor characterized by a low surface tension and viscosity, the droplets can easily spread on the substrate reducing then the vertical growth normal to the substrate and leading to a smoother film with small grain size. Figures 4 and 5 are a correlation between the solution viscosity and surface tension with the grain size of the formed film. As can be deduced, using a salt solution with large viscosity or surface tension leads to the formation of rough film with large grain size and crystallite size. The same conclusion has been outlined in a previous work [18] in ZnO thin film grown by ultrasonic spray pyrolysis.

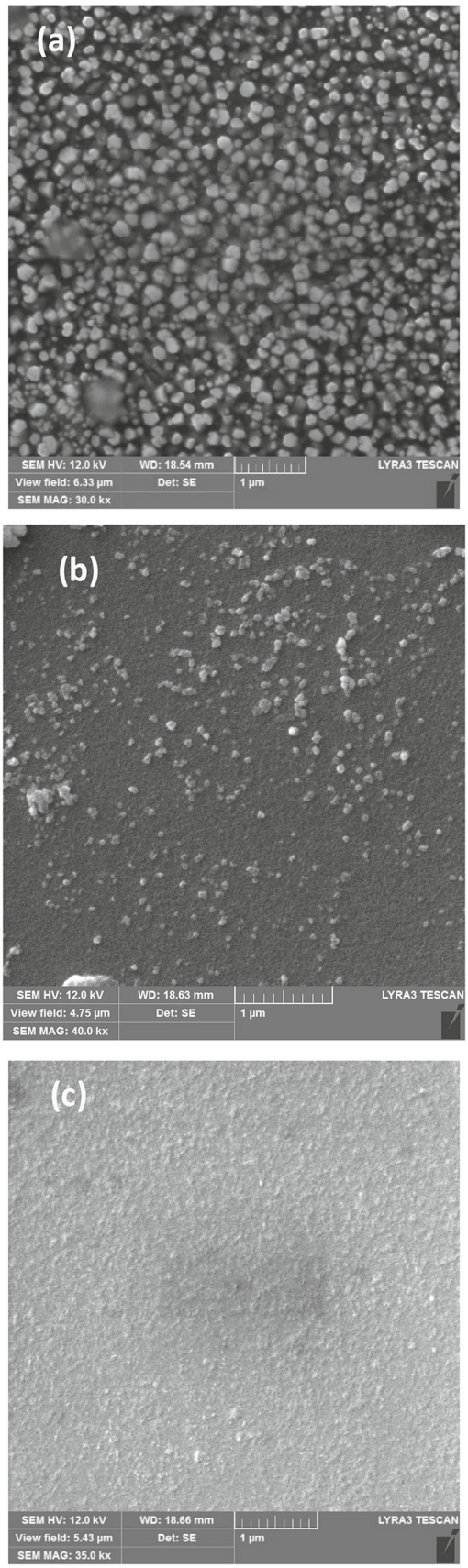

Fig. 3 SEM image of the ZnO thin films prepared with the three different zinc salt source **a** Zinc chloride, **b** Zinc nitride and **c** Zinc acetate

Table 2 The surface tension, viscosity and particle size D of ZnO thin films

Solution	Surface tension (N/m)	Viscosity (mPa.s)	*D* (nm)
Chloride	75	0.92	187.5
Nitrate	70	0.89	33.3
Acetate	57	0.85	21.7

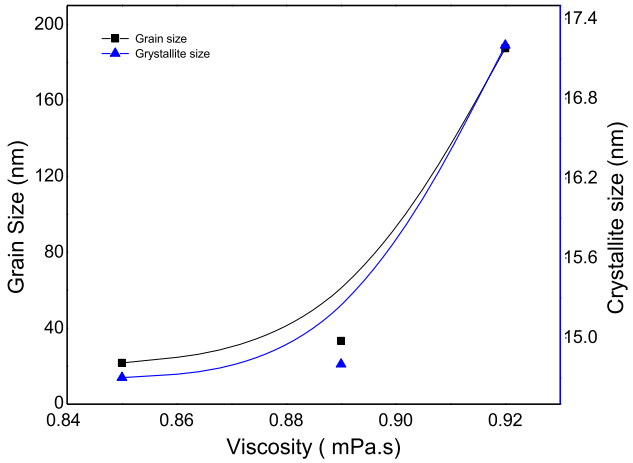

Fig. 4 Variation of the particle size and crystallite size in ZnO thin films as a function of the used solution viscosity of the three zinc sources

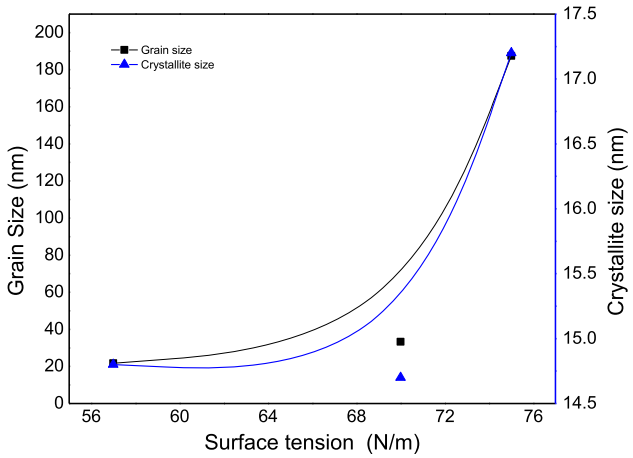

Fig. 5 Variation of the particle size and crystallite size in ZnO thin films as a function of the used solution surface tension of the three zinc sources

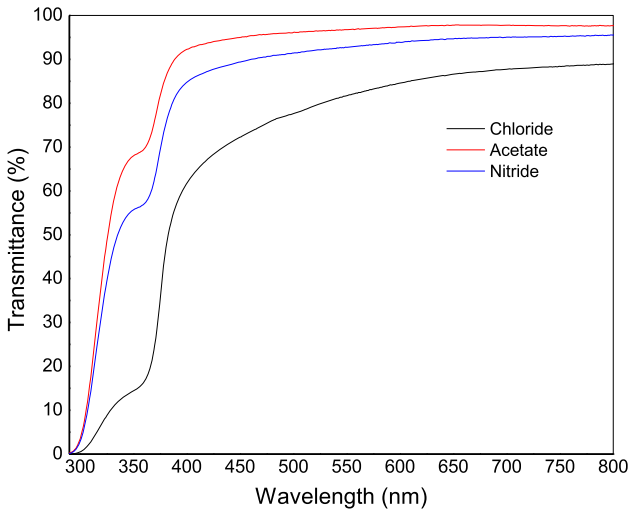

Fig. 6 UV–visible transmittance spectrum of ZnO thin films prepared with different salts source

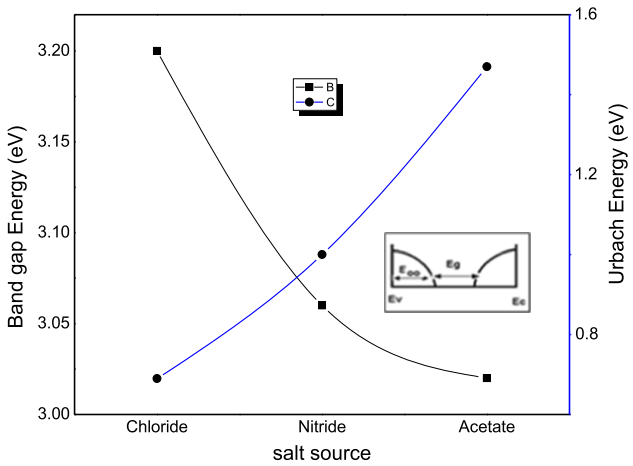

Fig. 7 Optical band gap and Urbach tail energy measured in films prepared with different salt sources. Insert a schematic drawn showing the optical band gap and Urbach energy in semiconductor band diagram

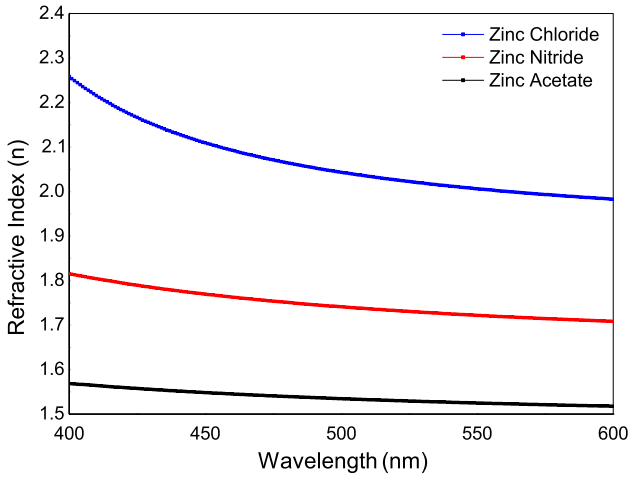

Fig. 8 The refractive index (n) of ZnO films prepared with different zinc salt source

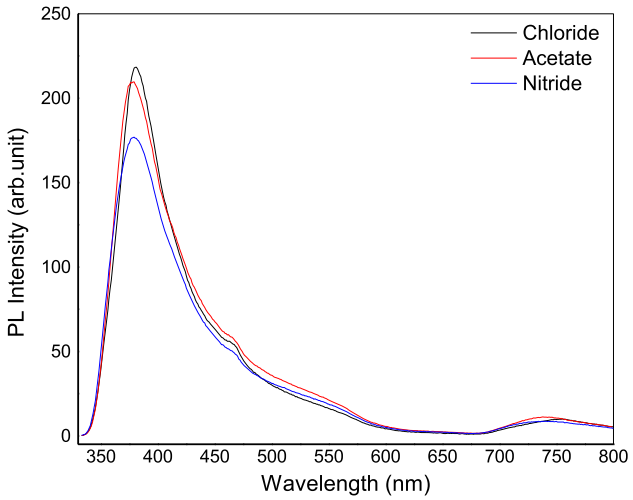

Fig. 9 PL emission spectra of ZnO thin films prepared with different zinc salt precursor

3.3 Optical properties

An UV/VIS spectrophotometer was used to study the optical transmittance of the prepared ZnO films with different precursors. Figure 6 shows the recorded optical transmission in different films in the wavelength range of 360–800 nm. As can be seen, the whole films exhibit a large transmittance ranged from 80 to 97% for the visible wavelengths. The film prepared with zinc acetate has the highest transparency (97%) regarding the ones prepared using zinc nitride and zinc chloride. This discrepancy is ascribed to the difference in the film morphology and the grain size. As deduced from SEM observations films prepared with zinc acetate

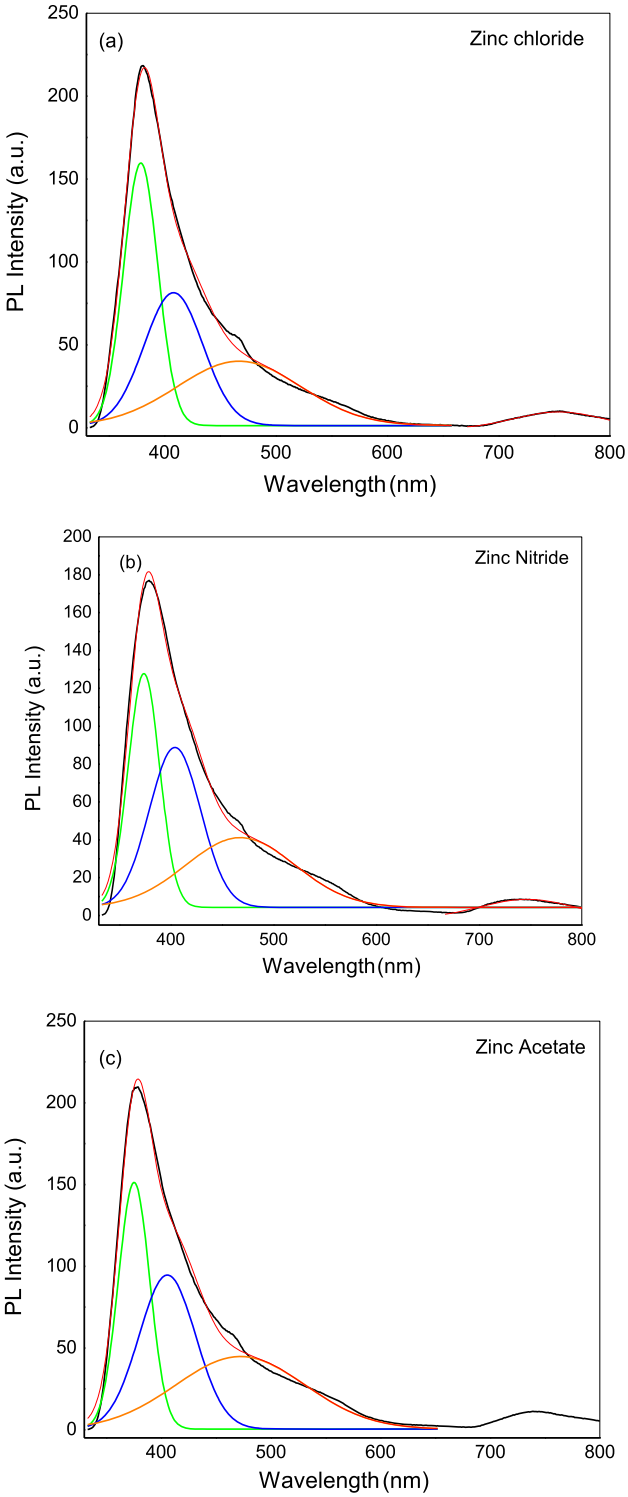

Fig. 10 Deconvolution of the PL spectra recorded in different ZnO thin films prepared with the three studied zinc salt source

are smooth, owing a small grain size, while films prepared with chloride and nitrite have a rough surface and lager grain size. It is well-known, that rough surfaces cause light scattering reducing then the films transmittance.

The optical band gaps of films were calculated using the Tauc formula [28]. Plotting $(\alpha h\upsilon)^2$ vs (hν), α is the absorption coefficient and hν is the photon energy, leads to the optical band gap values. The disorder in the film network is characterized by the band tail width called Urbach tail E_{oo} [29]. The latter can be estimated from the slop of the plot the plot of ln(α) versus (hν). In Fig. 7 we have plotted the calculated band gap along with Urbach energy in films prepared with different salt source.

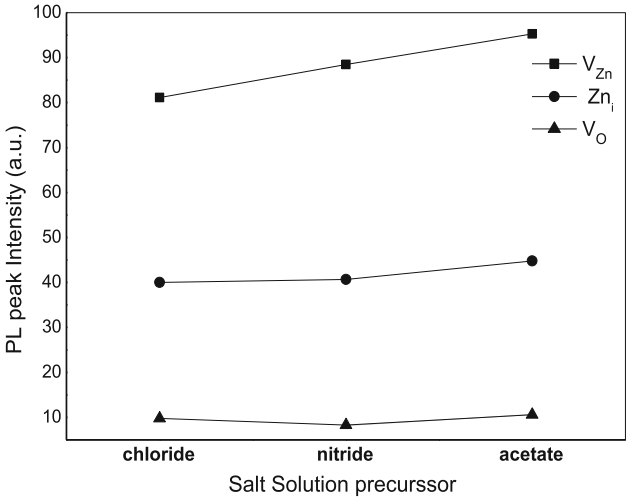

Fig. 11 Dependence of the three electronic defects intensity detected in ZnO thin films on the used zinc salt sources

As one can deduce, the film's optical band gap varies oppositely to the disorder. This is consistent with the fact that the reduction in the Urbach band energy i.e. tail band width causes the film's optical band gap broadening as depicted in inset Fig. 7. Chloride salt yields to film with less disorder and consequently larger band gap. In contrary, zinc acetate leads to highly disordered ZnO thin film with lower band gap. We inferred thereafter, that salt source nature controls the optical properties of ZnO, among each other parameters such as substrate temperature [12] and salt concentration [30].

Figure 8 shows the dispersive function of the refractive index of different films deduced from the transmittance measurements. As shown, the film prepared with zinc chloride have the largest refractive. This suggest that the film prepared with chloride is denser compared to ZnO thin films grown with zinc nitrate and zinc acetate. This is consistent with the low disorder calculated in this film (Fig. 7) and the high crystallinity of this film. Moreover, the high surface tension and viscosity of zinc chloride salt solution is at the origin of the film densification due to the solution retention and low spreading on the substrate surface. This is due to the fact that large viscosity and surface tension hinder the liquid motion and droplet spreading.

3.4 Photoluminescence

The photoluminescence emission spectra of all the samples recorded at room temperature in the wavelength range 340–800 nm are shown in Fig. 9. As shown, the whole ZnO films spectra are composed of UV emission characterized by a strong peak located at the 381 nm. A near infrared small peak located at around 750 nm, appears in all films spectra. This peak is due to the second-order of the UV emission band [31, 32].

In order to have a clear insight on the PL emission composition, each peak was decomposed by using a Gaussian deconvolution (Fig. 10a–c).

The fitting results shows that the spectrum of each peak consists of four peaks. A strong peak located at 3.25 eV is due to band-to-band transition, this peak energy is comparable to the calculated band gap in different films. A second peak located at 3 eV, according to the literature, this peak is attributed to zinc vacancies (V_{Zn}) [33, 34]. The third peak located at 2.6 eV assigned to the transition from a shallow donor (Zn_i) to a deep acceptor (V_{Zn}) [35]. The last one located at 1.67 eV attributed to the (V_O) defects in ZnO thin films [34].

In Fig. 11, we have regrouped the variation of different peaks intensity related to the electronic defects in films as a function of the starting solution salt source. As can be seen, the zinc vacancy is the most dominant defect in all films. This defect is slightly larger in the film prepared with zinc acetate, while the other defects such as Zn_i, and V_o are almost the same in all films.

4 Conclusion

In the present work, we have investigated the nature of the zinc salt source on the properties of ZnO thin films prepared by spray pyrolysis. We have addressed a correlation between the used solution properties such viscosity and surface tension with the properties of the grown films. We concluded that the effect of slat source is through the viscosity and surface tension of the prepared solution. A salt solution owing high solution viscosity or surface tension, such zinc chloride, leads to dense films with better crystallinity, larger grain size, less disorder and weak transparency due to the surface roughness. However, salt solution owing low viscosity and surface tension such as zinc acetate yields to a film with inferior crystallinity, smaller grain size, large disorder and higher transparency due to the resulted smooth surface. This discrepancy is explained in terms of the effect of viscosity and surface tension on droplets

motion and spreading on the substrate surface. The Pl analysis reveals that the salt source has fewer effect on the electronic defects in ZnO band gap.

Authors' contribution AAR and MSA carried out the experiment and wrote the manuscript with the support of AAM. ARA contributes in the sample preparation and structural characterization.

Data Availability Statement This manuscript has associated data in a data repository. [Authors' comment: The datasets analyzed during the current study are available from the corresponding author on reasonable request.]

Declarations

Conflict of interest There is no potential conflicts of interest. There are no relevant financial or non-financial competing interests to report.

References

1. T. Prasada Rao, M.C. Santhoshkumar, Effect of thickness on structural, optical and electrical properties of nanostructured ZnO thin films by spray pyrolysis. Appl. Surf. Sci. **255**, 4579–4584 (2009). https://doi.org/10.1016/j.apsusc.2008.11.079
2. M. Suchea, S. Christoulakis, K. Moschovis, N. Katsarakis, G. Kiriakidis, ZnO transparent thin films for gas sensor applications. Thin Solid Films (2006). https://doi.org/10.1016/j.tsf.2005.12.295
3. F. Michelotti, A. Belardini, A. Rousseau, A. Ratsimihety, G. Schoer, J. Mueller, Use of sandwich structures with ZnO:Al transparent electrodes for the measurement of the electro-optic properties of standard and fluorinated poled copolymers at $\lambda = 1.55$ μm. J. Non. Cryst. Solids. **352**, 2339–2342 (2006). https://doi.org/10.1016/J.JNONCRYSOL.2006.03.042
4. J. Hüpkes, B. Rech, O. Kluth, T. Repmann, B. Zwaygardt, J. Müller, R. Drese, M. Wuttig, Surface textured MF-sputtered ZnO films for microcrystalline silicon-based thin-film solar cells. Sol. Energy Mater. Sol. Cells. **90**, 3054–3060 (2006). https://doi.org/10.1016/J.SOLMAT.2006.06.027
5. C. Besleaga, G.E. Stan, A.C. Galca, L. Ion, S. Antohe, Double layer structure of ZnO thin films deposited by RF-magnetron sputtering on glass substrate. Appl. Surf. Sci. **258**, 8819–8824 (2012). https://doi.org/10.1016/J.APSUSC.2012.05.097
6. W. Lee, M.C. Jeong, J.M. Myoung, Catalyst-free growth of ZnO nanowires by metal-organic chemical vapour deposition (MOCVD) and thermal evaporation. Acta Mater. **52**, 3949–3957 (2004). https://doi.org/10.1016/J.ACTAMAT.2004.05.010
7. T. Pauporté, D. Lincot, Electrodeposition of semiconductors for optoelectronic devices: results on zinc oxide. Electrochim. Acta. **45**, 3345–3353 (2000). https://doi.org/10.1016/S0013-4686(00)00405-9
8. Z. Neng Ng, K. Yoong Chan, Z.-N. Ng, K.-Y. Chan, T. Tohsophon, Effects of annealing temperature on ZnO and AZO films prepared by sol–gel technique. Appl. Surf. Sci. **258**, 9604–9609 (2012). https://doi.org/10.1016/j.apsusc.2012.05.156
9. L. Moreno, C. Sánchez-Aké, M.B.-A.S. Science, undefined 2014, Double-beam pulsed laser deposition for the growth of Al-incorporated ZnO thin films, Elsevier. (n.d.). https://www.sciencedirect.com/science/article/pii/S0169433214000798. Accessed 19 Feb 2022.
10. W.J. Jeong, S.K. Kim, G.C. Park, Preparation and characteristic of ZnO thin film with high and low resistivity for an application of solar cell. Thin Solid Films **506–507**, 180–183 (2006). https://doi.org/10.1016/J.TSF.2005.08.213
11. P.P.-M.C. and physics, undefined 1999, Versatility of chemical spray pyrolysis technique, Elsevier. (n.d.). https://www.sciencedirect.com/science/article/pii/S0254058499000498. Accessed 19 Feb 2022.
12. A.S. Enigochitra, P. Perumal, C. Sanjeeviraja, D. Deivamani, M. Boomashri, Influence of substrate temperature on structural and optical properties of ZnO thin films prepared by cost-effective chemical spray pyrolysis technique. Superlattices Microstruct. **90**, 313–320 (2016). https://doi.org/10.1016/J.SPMI.2015.10.026
13. N. Lehraki, M.S. Aida, S. Abed, N. Attaf, A. Attaf, M. Poulain, ZnO thin films deposition by spray pyrolysis: influence of precursor solution properties. Curr. Appl. Phys. **12**, 1283–1287 (2012). https://doi.org/10.1016/j.cap.2012.03.012
14. A. El Hichou, M. Addou, J. Ebothé, M. Troyon, Influence of deposition temperature (Ts), air flow rate (f) and precursors on cathodoluminescence properties of ZnO thin films prepared by spray pyrolysis. J. Lumin. **113**, 183–190 (2005). https://doi.org/10.1016/J.JLUMIN.2004.09.123
15. S. Kurtaran, Al doped ZnO thin films obtained by spray pyrolysis technique: influence of different annealing time. Opt. Mater. (Amst.) **114**, 110908 (2021). https://doi.org/10.1016/J.OPTMAT.2021.110908
16. S.S. Shinde, A.P. Korade, C.H. Bhosale, K.Y. Rajpure, Influence of tin doping onto structural, morphological, optoelectronic and impedance properties of sprayed ZnO thin films. J. Alloys Compd. **551**, 688–693 (2013). https://doi.org/10.1016/J.JALLCOM.2012.11.057
17. E. Bacaksiz, M. Parlak, M. Tomakin, A. Özçelik, M. Karakiz, M. Altunbaş, The effects of zinc nitrate, zinc acetate and zinc chloride precursors on investigation of structural and optical properties of ZnO thin films. J. Alloys Compd. **466**, 447–450 (2008). https://doi.org/10.1016/j.jallcom.2007.11.061
18. M. Khammar, S. Guitouni, N. Attaf, M.S. Aida, A. Attaf, Effect of thermo-physical properties of Zn precursors on ZnO thin films grown by ultrasonic spray. Ceram. Int. **43**, 9919–9925 (2017). https://doi.org/10.1016/j.ceramint.2017.04.179
19. F. Baig, M.W. Ashraf, A. Asif, M. Imran, A comparative analysis for effects of solvents on optical properties of Mg doped ZnO thin films for optoelectronic applications. Optik-Int. J. Light Electron Opt. **208**(2), 164534 (2020)
20. D. Poelman, P.F. Smet, Methods for the determination of the optical constants of thin films from single transmission measurements: a critical review. J. Phys. D: Appl. Phys. **36**, 1850 (2003)
21. G.B. Harris, Quantitative measurement of preferred orientation in rolled uranium bars. Lond. Edinb. Dublin Philos. Mag. J. Sci. **43**, 113–123 (2009). https://doi.org/10.1080/14786440108520972
22. V. Darakchieva, Strain-related structural and vibrational properties of group-III nitride layers and superlattices 2004. (n.d.). https://www.diva-portal.org/smash/record.jsf?pid=diva2:1595053. Accessed 24 Feb 2022.
23. C.G. Pope, X-ray diffraction and the Bragg equation. J. Chem. Educ. **74**, 129–131 (1997). https://doi.org/10.1021/ED074P129
24. H.F. Memurdie, M.C. Morris, E.H. Evans, B. Paretzkin, W. Wongng, C.R. Hubbard, Standard X-ray diffraction powder patterns from the JCPDS research associateship. Powder Diffr. **1**, 265–275 (1986). https://doi.org/10.1017/S0885715600011829

25. S. Mustapha, M.M. Ndamitso, A.S. Abdulkareem, J.O. Tijani, D.T. Shuaib, A.K. Mohammed, A. Sumaila, Comparative study of crystallite size using Williamson-Hall and Debye-Scherrer plots for ZnO nanoparticles. Adv. Nat. Sci. Nanosci. Nanotechnol. **10**, 045013 (2019)
26. H. Bendjedidi, A. Attaf, H. Saidi, M.S. Aida, S. Semmari, A. Bouhdjar, Y. Benkhetta, Properties of n-type SnO_2 semiconductor prepared by spray ultrasonic technique for photovoltaic applications. J. Semicond. **36**, 123002 (2015)
27. I.B. Kherchachi, A. Attaf, H. Saidi, A. Bouhdjer, H. Bendjedidi, Y. Benkhetta, R. Azizi, Structural, optical and electrical properties of Sn_xS_y thin films grown by spray ultrasonic. J. Semicond. **37**, 032001 (2016). https://doi.org/10.1088/1674-4926/37/3/032001
28. J.J Tauc Amorphous and liquid semiconductors.Ed: Plenum, London, (1974)
29. F. Urbach, Phys. Rev. **92**, 1324 (1953)
30. D. Bao, H. Gu, A. Kuang, Sol-gel-derived c-axis oriented ZnO thin films. Thin Solid Films **312**, 37–39 (1998). https://doi.org/10.1016/S0040-6090(97)00302-7
31. M. Wang, E.J. Kim, E.W. Shin, J.S. Chung, S.H. Hahn, C. Park, Low-temperature solution growth of high-quality ZnO thin films and solvent-dependent film texture. J. Phys. Chem. C **112**, 1920 (2008)
32. M. Wang, E.J. Kim, S.H. Hahn, Photoluminescence study of pure and Li-doped ZnO thin films grown by sol–gel technique. J. Lumin. **131**, 1428 (2011)
33. K.S. Harshavardhan, S. Rajagopalan, L.K. Malhotra, K.L. Chopra, Photoinduced changes in the Urbach tail in Ge- and As-based chalcogenide glasses. J. Appl. Phys. **54**, 1048 (1998). https://doi.org/10.1063/1.332108
34. A. Gadallah, M.E.-N.-A. in C.M. Physics, undefined 2013, Structural, optical constants and photoluminescence of ZnO thin films grown by sol-gel spin coating, Hindawi.Com. (n.d.). https://www.hindawi.com/journals/acmp/2013/234546/. Accessed 14 Apr 2022.
35. D. Behera, B.S. Acharya, Nano-star formation in Al-doped ZnO thin film deposited by dip-dry method and its characterization using atomic force microscopy, electron probe microscopy, photoluminescence and laser Raman spectroscopy. J. Lumin. **128**, 1577–1586 (2008). https://doi.org/10.1016/J.JLUMIN.2008.03.006